Astron. Astrophys. 317, 712–722 (1997)

ASTRONOMY
AND
ASTROPHYSICS

The 1978–1995 variability of the symbiotic star AG Pegasi in the ultraviolet⋆

Aldo Altamore[1] **and Angelo Cassatella**[2]

[1] Dipartimento di Fisica E. Amaldi, Universitá degli Studi di Roma Tre, Via della Vasca Navale 84, I-00146 Roma, Italy
[2] Istituto di Astrofisica Spaziale, CNR, Via E. Fermi 21, I-00044 Frascati, Italy

Received 23 February 1996 / Accepted 13 June 1996

Abstract. In this paper we study in detail the variability of the symbiotic nova AG Peg in the IUE range during the period 1978–1995. We find that the luminosity of the hot component decreased steadily from about 1850 $L_\odot$ in 1978 to 430 $L_\odot$ in 1995 while its effective temperature remained nearly constant, $86500 \pm 1300\ ^\circ K$. At the same time, the mass loss rate decreased by a factor of 4-5 although the ejection velocity remained constant. The observed fainting of both the narrow and the broad emission lines is ascribed to the decrease of the luminosity and ionizing flux from the hot source. The narrow emission lines and the long wavelength UV continuum show periodic variations arising from a dense and asymmetric nebular region associated with the cool star. Radial velocity variations of the narrow lines indicate that this region is receding from the center of mass of the system, and support the presence of the ablation tail suggested by Penston and Allen (1985). No periodic flux variations are seen in the short wavelength ultraviolet continuum and in the broad emission lines, which are both formed in the fast wind from the hot component.

Key words: stars: individual: AG Peg – cataclysmic variables – binaries: symbiotic – ultraviolet: stars – line: profiles

1. Introduction

One of the earliest and most important contributions of the International Ultraviolet Explorer (IUE) to the study of symbiotic stars was to provide evidence for their binary nature, inferred from the strong emission lines and continuum observed at ultraviolet wavelengths. Detailed analyses of these data have allowed to clarify the nature of the hot components, which were found to be mostly located in the region of the HR diagram occupied by the hot nuclei of planetary nebulae or by white dwarfs, with temperatures of the order of $10^5\ ^\circ K$ and luminosities of the order of 10 to $10^4\ L_\odot$ (see Mürset et al. 1991; Mürset and Nussbaumer 1994; and references therein).

Using IUE data accumulated over many years it has been possible to study the behaviour of symbiotic stars during outburst (see e.g. Cassatella et al. 1992a; Fernández Castro et al. 1995) and quiescence. Symbiotic stars in quiescence usually show regular and phase-related variations of the emission line fluxes and of the nebular continuum. These variations are ascribed to the combined effects of orbital motion and asymmetry of the nebular region, as in the case of Z And (Fernandez-Castro et al. 1988, 1995), AG Dra (Viotti et al. 1984) and BF Cygni (González-Riestra et al. 1990).

Recent work has been dedicated to model how the stellar wind from the hot primary interacts with the one from the cool secondary component to modify the density and ionization structure of the nebular region (Nussbaumer & Walder 1993, and references therein). Because of the quite large wind velocity from the hot component (Penston & Allen 1985), the symbiotic nova AG Peg (HD 207757) is a primary laboratory to study the phenomenology of colliding winds.

AG Peg has been in quiescence until 1850 and then slowly brightened by 3 magnitudes reaching magnitude 6 at maximum in 1855. A description of these early phases can be found in Boyarchuk (1967 and references therein). The further evolution was characterized by a slow decay. By 1995, with $V \simeq 8.5$, the star has nearly returned to its pre-outburst visual luminosity. The binary nature of AG Peg, suggested by Boyarchuk (1967), was confirmed by Cowley and Stencel (1973) who, on the basis of radial velocity variations of the M giant secondary, found a binary period of about 830 days. The first evidence for the presence of a hot companion was provided by the OAO-2 observations by Gallagher et al. (1979). The basic interpretation of the ultraviolet spectrum of AG Peg is given by Penston and Allen (1985). These authors identify "a 900 km s^{-1}P Cygni mass loss wind from the hot component" as well as a low velocity and high density region associated with the cool M giant companion, and suggest that this latter emission region "includes a tail of gas

Send offprint requests to: A. Altamore
Tables 2 to 5 only available in electronic form via ftp edsarc.u-straby.fr or ftp. 130.79.128.5
⋆ Based on observations by the International Ultraviolet Explorer collected at the Villafranca Satellite Tracking Station of the European Space Agency or obtained from the IUE Data Bank.

ablated from the giant by the intense ultraviolet radiation field and hot wind". Recent ROSAT observations by Mürset, Jordan & Walder (1995) strongly support the presence of shock-heated plasma in AG Peg.

In this paper we analyse and discuss the IUE observations of AG Peg so far available to study the long term evolution of the emission lines and of the continuum, as well as the changes of the mass loss rate and of the bolometric luminosity over the period 1978-1995.

2. Basic parameters of AG Peg

According to the most recent determination of the orbital parameters by Kenyon et al. (1993), the orbital period of AG Peg is 812.3 days, the binary separation is 2.5 ± 0.1 AU (for an inclination $i = 50°$) and the masses of the M3 giant secondary and of the hot primary are $M_g = 2.6 \pm 0.4\ M_\odot$ and $M_h = 0.65 \pm 0.10\ M_\odot$, respectively. The orbital period reported by Kenyon et al. (1993) is in good agreement with the photometric period determined by Fernie (1985), who found the following ephemeris: $T_m = 2442710.1 + 816.5E$ (days), being T_m the Julian date of visual maxima and E the orbital cycle. In the following we will adopt the photometric ephemeris by Fernie (1985) and the orbital elements by Kenyon et al. (1993).

For the distance to AG Peg we will adopt the value of 650 pc given by Mürset et al. (1991), and for the reddening we take the value E(B-V) = 0.12 suggested by Penston and Allen (1985). The reddening correction was performed according to the extinction law by Seaton (1979).

3. Observations

The present study is based on the best quality low and high resolution spectra of AG Peg obtained with IUE in the period from July 1978 to May 1995. Particular care was taken to improve the homogeneity of data extraction and calibration of the observations, and the accuracy of the measurements of continuum fluxes, line fluxes and equivalent widths.

The Log of the IUE observations is given in Table 1. The table shows that the object was regularly monitored by IUE until December 1981; after a gap of several years in which just a few observations were obtained, a new phase of regular monitoring started in September 1989 and continued until May 1995. Most of the data taken after November 1990 were obtained under our observing programmes.

The IUE low resolution spectra were calibrated according to Holm et al. (1982) for the SWP and LWR cameras, and to Cassatella et al. (1992b) for the LWP camera. The IUE high resolution spectra were calibrated according to Cassatella et al. (1994). The archival data, if processed with an obsolete version of the IUE Spectral Image Processing Software, were reprocessed to avoid systematic errors in the flux calibration and in the wavelength scale. A special care was taken to exclude data affected by instrumental effects (e.g. saturation, bright spots in the cameras, reseau marks). The data analysis was carried out using the computer facilities of the Istituto Astronomico of the University La Sapienza, Rome.

4. The UV continuum

The ultraviolet continuum of AG Peg is dominated by radiation from the hot source at short wavelengths, and from gas recombination continuum at longer wavelengths. To study these two components separately, we have selected two continuum bands 30 Å wide centered around 1455 Å and 1835 Å, where the hot source is dominant, and one band 30 Å wide centered around 2885 Å, where the recombination continuum dominates over the emission from the hot star (see also Sect. 7). The three bands were selected for being reasonably free from contamination by nearby emission lines. The corresponding measurements of the continuum fluxes (not corrected for reddening) are reported in Table 2 and plotted as a function of time in Fig. 1a,b,c. In the table and in Fig. 1d we show also, for comparison, the visual magnitude m_{FES} as derived from the counts of the Fine Error Sensor (FES) on board IUE by applying the FES calibration by Barylak (1989). As expected, the FES light curve is in agreement with the Fernie's ephemeris, whose photometric maxima are marked with vertical bars in the figure. It appears from Fig. 1a,b that, in the period 1978 - 1995, the continuum of AG Peg has faintened by about 1.8 mag in the 1455 Å band and by about 1.5 mag in the 1835 Å band. No periodic phase-related modulations were seen in these short wavelength bands.

The 2885 Å band shows a less pronounced steady decay but, unlike the bands at 1455 Å and 1835 Å, important modulation effects in phase with the Fernie's ephemeris are clearly seen superimposed to the secular decay (see Fig. 1c). Although based on considerably less significant amount of data in terms of orbital cycle coverage, also Kenyon et al. (1993) reached a similar conclusion for the long wavelength band at 3275 Å .

As discussed later in more detail, the unmodulated slow decay of the short wavelengths fluxes is due to a decrease of the luminosity and ionizing flux of the hot component, while the phase dependent changes of the nebular continuum and of the narrow emission lines arise from a region near the cool component which is photoionized by the hot companion.

5. The emission lines

The profiles and fluxes of the UV emission lines in AG Peg have shown large variations over the last 17 years. To study these variations in more detail we take as reference the work of Penston and Allen (1985), which describes the situation in 1979. These authors distinguish between three classes of emission lines:

i) lines showing only a narrow component, like SiIV 1400 Å, OIII] 1660 Å, NIII] 1750 Å, SiIII] 1893 Å, and CIII] 1909 Å, the full width at half maximum (FWHM) of these lines being about 65 km s^{-1};

ii) broad lines showing a P Cygni profile, as the resonance doublets of NV 1240 Å and CIV 1550 Å, as well as the HeII 1640 Å

Table 1. Log of the IUE observations of AG Peg

Date	J.D.	Images
27 Jul 78	3717	SWP02123
18 Aug 78	3739	LWR02101 SWP02325 SWP02326* SWP02334*
13 Oct 78	3795	LWR02591* SWP02953*
4 Nov 78	3827	SWP03342 SWP03342
4 Jan 79	3877	LWR03375 LWR03376 SWP03795 SWP03796
6 Jan 79	3880	SWP03830
29 Jun 79	4054	SWP05669* LWR04914* LWR04915 SWP05670 SWP05670 LWR04915
21 Jul 79	4076	LWR05137 SWP05882
2 Sep 79	4118	SWP06353* LWR05489* SWP06354 LWR05490 SWP06354 SWP06355*
15 Sep 79	4132	LWR05596* SWP06527*
9 Oct 79	4156	SWP06809*
14 Dec 79	4222	LWR06389* SWP07406* LWR06390 SWP07407 LWR06390
14 Apr 80	4344	SWP08760* LWR07504*
23 May 80	4383	LWR07834 LWR07834 SWP09087*
25 May 80	4385	SWP09117
30 Jul 80	4451	LWR08390* SWP09643
23 Oct 80	4536	LWR09129 SWP10454* LWR09130* SWP10455
9 Jan 81	4614	LWR09672* SWP11004* LWR09673 SWP11005
10 May 81	4735	LWR10571* SWP13957*
4 Dec 81	4943	LWR12079 SWP15649* SWP15650 SWP15651*
27 May 85	6213	LWP06070 LWP06070 SWP26023
12 Dec 86	6777	SWP29862* LWP09698* SWP29863*
16 Sep 89	7786	SWP37046*
21 Oct 89	7821	SWP37419 SWP37420* LWP16594
28 Oct 89	7828	SWP37476* LWP16684* SWP37477*
20 Nov 90	8216	SWP40147 LWP19252 SWP40148* LWP19253* SWP40149*
2 Aug 91	8471	SWP42159 LWP 2093
4 Nov 91	8565	SWP43005 LWP21634 SWP43006* LWP21635* SWP43007*
25 Oct 92	8921	SWP46060* LWP24149* SWP46061
6 Nov 92	8932	LWP24280* SWP46142*
20 May 93	9127	LWP25564 SWP47696 LWP25564 SWP47697* LWP25565
24 Jul 93	9192	LWP25993* SWP48230* SWP48231* LWP25994 SWP48232 LWP25595*
25 Sep 93	9255	SWP48713* LWP26447 SWP48714 LWP26448*
12 May 94	9485	LWP28121 SWP50752* SWP50753 LWP28122*
12 Oct 94	9638	LWP29383 SWP52385* SWP52386 SWP52387*
25 May 95	9863	SWP54747 LWP30768 SWP54748* SWP54749*

Note: High resolution images are labeled with $*$

and NIV 1718 Å lines. These broad lines provide evidence for a fast wind flowing out from the hot source at a velocity of about 900 km s^{-1}.

iii) lines showing composite profiles where both the narrow and the broad components are present, like NIV] 1487 Å.

By studying the profile and flux changes of the emission lines it is possible to gain information about the regions where the the narrow and broad components are formed, as shown in the following.

5.1. The narrow lines

The flux variations of all the narrow lines follow a very similar pattern. As a representative example we take the SiIII] 1893 Å and CIII] 1909 Å lines, whose fluxes are listed in Table 3a and plotted as a function of time in Fig. 2a,b (vertical bars, as in Fig. 1, correspond to the visual maxima). It appears clearly that the fluxes of the narrow emission lines vary in phase with the visual and the 2885 Å fluxes, suggesting formation in a common emitting region associated with the cool component. This result is consistent with previous observations of symbiotic stars in quiescence, which indicate that both the nebular continuum and the narrow emission lines are formed in the extended atmosphere and wind of the cool giant, photoionized by the hot companion (see e.g. Munari 1989; Fernández-Castro et al. 1995, and references therein).

Even stronger phase-dependent variations are shown by the flux ratio CIII]/SiIII], given in Fig. 2c, which is very sensitive to the electron density. The electron density N_e can actually be determined by comparing the observed CIII]/SiIII] ratio with

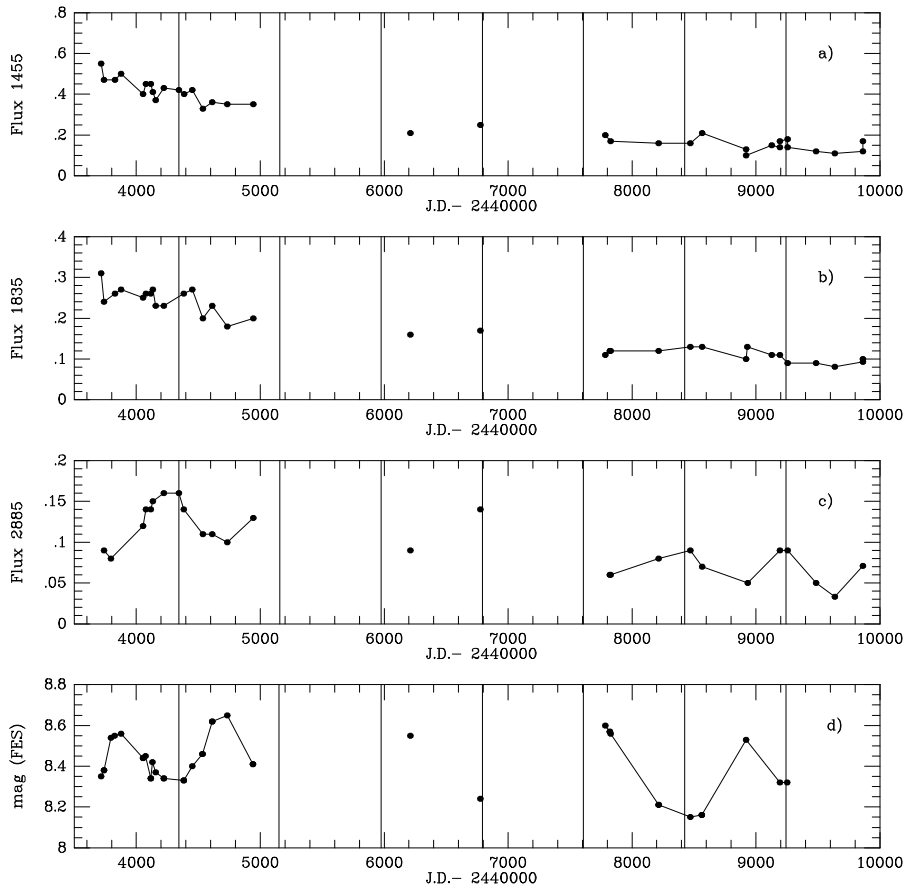

Fig. 1a–d. Observed fluxes at 1445 Å, 1885 Å, 2885 Å and FES magnitude as a function of Julian date. Vertical bars denote the times of photometric maxima according to Fernie (1985). Fluxes are in units of 10^{-11} erg cm^{-2} s^{-1}A^{-1}.

the computed ratio of the corresponding emissivities (see Nussbaumer and Stencel 1987), provided the relative abundance by number of Silicon to Carbon $a = N(Si)/N(C)$ and the fractional abundance of these elements in the doubly ionized state, $f = [N(Si^{2+})/N(Si)]/[N(C^{2+})/N(C)]$ are known. Adopting $a = 0.1$ (solar abundance) and $f = 0.1$ we can derive the electron densities listed in Table 3a and shown as filled dots in Fig. 2d.

Here, the implicit approximation made is that the SiIII] and CIII] emissions are formed in the same region. Although this assumption is only roughly true (c.f. Nussbaumer and Vogel 1989), this does not affect the general aspects of our conclusions. As shown in Fig. 2d, also the electron density appears to vary with time, showing prominent maxima and minima which closely correspond to the ones of the visual light curve.

More precise electron density determinations, not relying on the approximation that the CIII] and SiIII] regions coincide, can be obtained from the flux ratios of lines belonging to the NIII] 1750 Å quintuplet, which are well separated in IUE high resolution spectra. We have selected ten SWP spectra where the strongest components at 1748.63 Å , 1749.64 Å , and 1753.96 Å of the quintuplet were sufficiently well exposed and measured the flux ratio $I(1748.63)/I(1749.64)$ and $I(1753.96)/I(1749.64)$. Using these ratios and a code for detailed statistical equilibrium calculations provided by Howarth, Adams and Snijders (1993) we have then derived the electron densities listed in Table 3b. These values (open dots in Fig. 2d) are in agreement with the ones derived from the low resolution fluxes of the CIII] and SiIII] lines (filled dots).The electron density derived are anyhow close to the determinations by Penston and Allen (1985) for the same epoch.

It is clear from Figs. 1 and 2, that the flux of the narrow emission lines and the flux at 2885 Å (mostly due to the recombination continuum) show a strong and direct correlation with the electron density and with the visual flux (mostly due to the M giant). The reported flux variations can be understood as due to variations, during orbital motion, of the projected mean electron density along the line of sight of an asymmetric emitting region associated with the red giant companion. Additional information on this region are given in Sect. 6.

5.2. The broad lines

According to Vogel and Nussbaumer (1994), the mass loss rate from the hot component of AG Peg has decreased by about a factor of 4 from 1978 to 1993. In this section we address the question whether the reported mass loss variation is due to a decrease of the expansion velocity in the wind or to a decrease of the density of the ejected matter.

Recent observations with the GHRS spectrograph on board the Hubble Space Telescope by Nussbaumer, Schmutz and Vogel (1995), show that the broad components in the NV

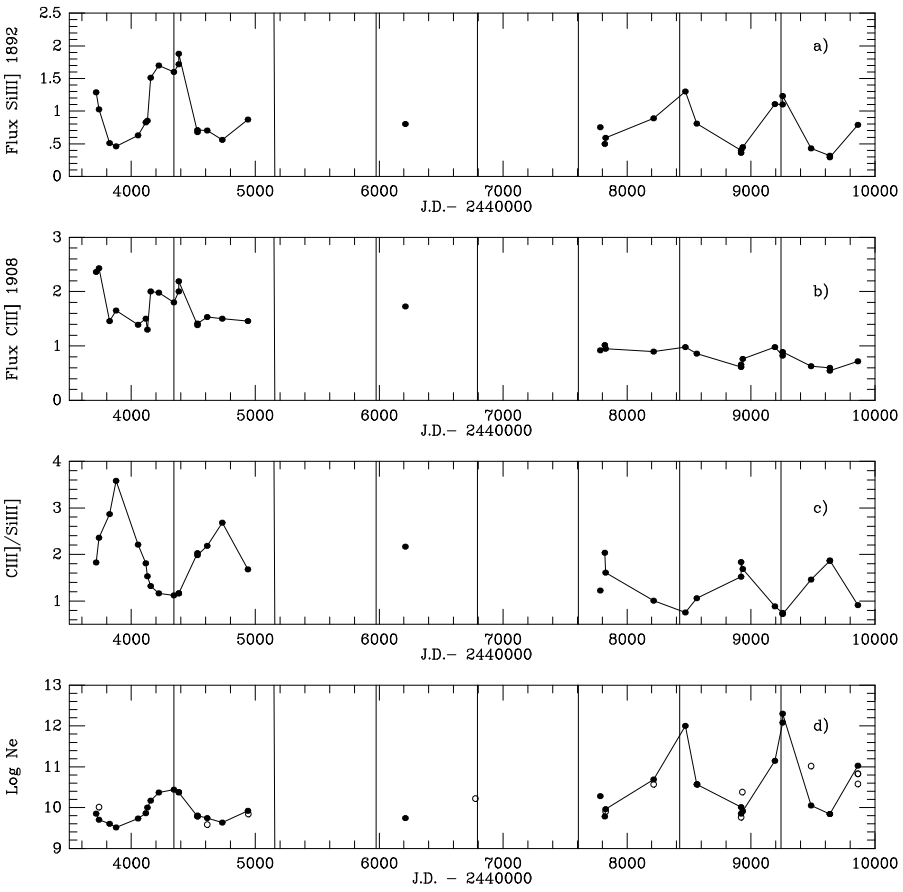

Fig. 2a–d. Panels **a**, **b** and **c** show the observed fluxes of the narrow lines SiIII] 1893 Å and CIII] 1909 Å and flux ratio SiIII]/CIII] as a function of Julian Date, respectively. Panel **d** shows the time variations of the electron density derived from SiIII]/CIII] ratio (filled dots) and from the NIII] multiplet (open dots). Vertical bars are as in Fig. 1. Fluxes are in units of 10^{-11} erg cm^{-2} s^{-1}.

1240 Å and HeII 1640 Å seen by Penston and Allen (1985) in 1979, were also present in June 1994 and had about the same width. Vogel and Nussbaumer (1994) also noticed that the broad components of the NV and HeII lines had a similar shape in 1979 and 1989.

In the following, we use the best quality IUE high resolution spectra to show that the FWHM of the broad components has actually remained constant all through the period 1978-1994. We have considered as the most suitable lines for this purpose the NIV] 1487 Å and the HeII 1640 Å lines because they: i) display a prominent broad component since the earliest observations in 1978, ii) are strong enough to be measured accurately, iii) are isolated. We have purposefully excluded the CIV] 1550 Å and the NV 1240 Å doublets because their components are radiatively coupled, given the observed large velocity field. We have also excluded the SiIV 1400 Å doublet because this feature is not strong enough for its broad component to be seen in IUE high resolution spectra.

The individual line profiles were analysed by fitting the observed spectra with a sum of two gaussian components plus a linear baseline representing the local continuum. This procedure allows one to optimize, with typically 4 or 5 iteration cycles, the peak intensity, central wavelength and full width at half maximum of the individual components. Some representative results are shown in Fig. 3a and 3b for HeII 1640 Å and NIV] 1486.5 Å, respectively. It is apparent from Fig. 3a that the broad component in the HeII feature, which completely dominates the profile in 1978, becomes fainter and fainter as time increases until the narrow component, not seen in 1978, emerges and eventually becomes dominant.

The results of the line profile fitting indicate that the full width at half maximum of the broad component has remained substantially constant within the observational errors during the period 1978 - 1995. The mean values are FWHM = 770 ± 40 km s^{-1} for HeII 1640 Å (20 measurements), and FWHM = 870 ± 100 km s^{-1} for NIV] 1486.5 Å (13 measurements). The averages refer to the period 1978 - 1994 for the HeII line and 1978 - 1985 for the NIV] line. After 1985 the broad component of the NIV] line becomes too faint to be measurable accurately. Such a component was also too faint to be clearly detectable with HST in 1994 (see Nussbaumer et al. 1995). Note that the smaller FWHM of the HeII emission, compared with that of NIV] is due to the presence of a P Cygni profile (see Fig. 6 and Sect. 6). These results, and in particular those relative to the HeII line, provide a strong support to the idea that the expansion velocity of the wind from the hot component has remained constant since 1978.

On the other hand, the strength of the broad components has decreased considerably during the same period. As it appears in Fig. 4 (filled dots), the decrease was by a factor of about 8 for the broad component of the HeII line, i.e. sensibly larger than for the narrow lines belonging to lower ionization species such as SiIII] and CIII] (see Fig. 2a,b). A direct comparison with the

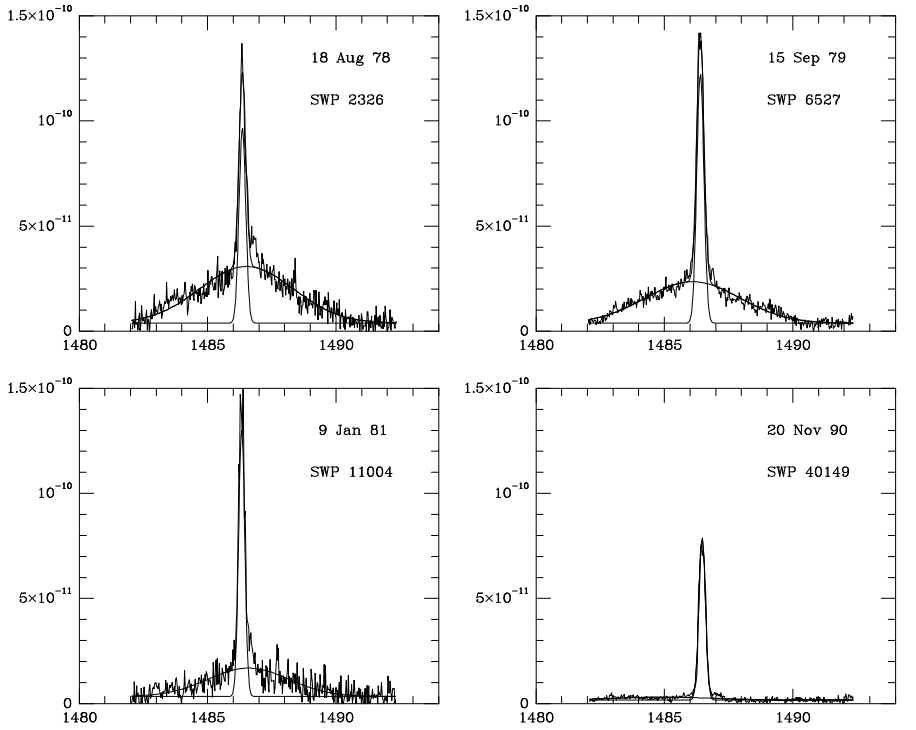

Fig. 3a. Line profile of the HeII 1640 Å line at four different dates. The observed profiles were fitted with one gaussian component for the earliest spectra of August 1978 and October 1979, and with two components for the later dates. It appears that the width of the broad component has remained constant, while the line flux has considerably decreased. Fluxes (observed) are in erg cm^{-2} $s^{-1}A^{-1}$.

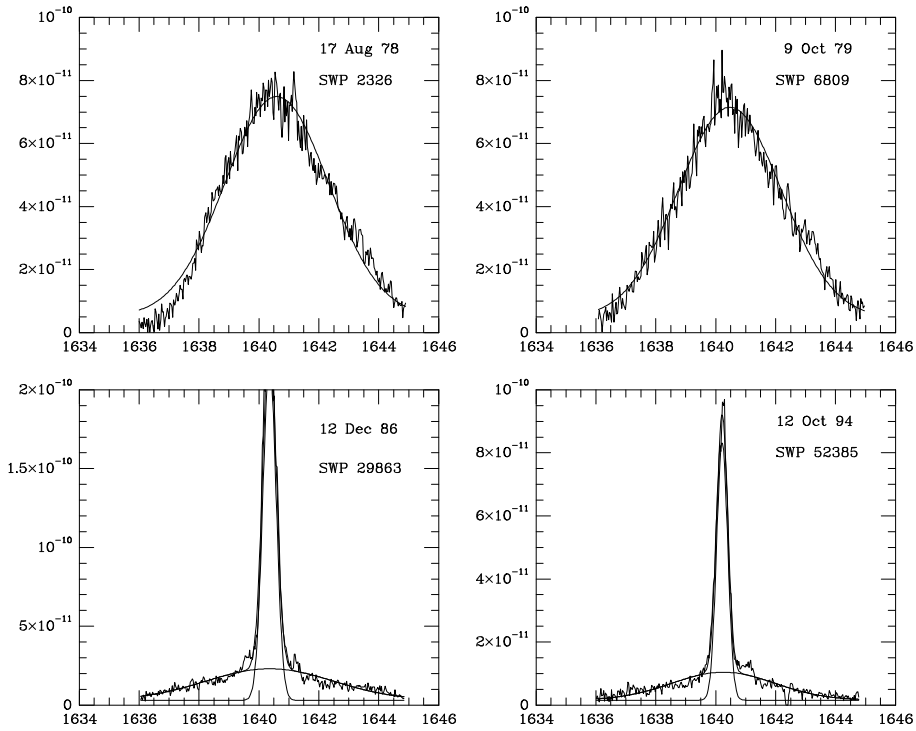

Fig. 3b. Same as Fig. 3a for the NIV] 1487 Å line. The four observed line profiles were in this case fitted with two components, indicated in the figure.

narrow component of the HeII line itself is more difficult, because this latter is not measurable in the earliest spectra (before JD-2440000 = 4600), and quite large errors (up to 30% - 50%) are to be attached to the measured fluxes at later dates until JD-2440000 = 7800.

As shown in Fig. 4, the fluxes of the HeII line do not present phase-dependent variations, contrary to what seen in the narrow lines (cf. Fig. 2a,b). The absence of any periodicity is consistent with the HeII line being formed in a symmetric region associated with the wind from the hot component, as confirmed by the radial velocity measurements described in the next Section.

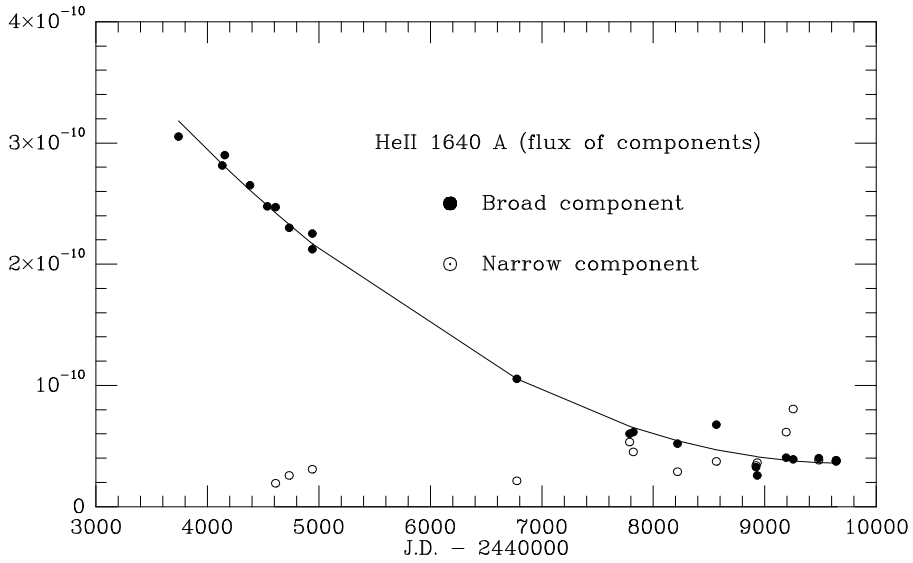

Fig. 4. Time variation of the broad and narrow component of the HeII 1640 Å line (filled and open dots, respectively). Fluxes (observed) are in erg cm^{-2} s^{-1}.

6. Radial velocities

The different behaviour of the narrow lines compared to the broad lines, in terms of variability and line profiles, reflects formation in different regions. Further information on the relevant line forming regions can be obtained from radial velocity measurements. Given the complexity of the line profiles, the central positions of the emission lines were determined via the gaussian fitting algorithm already mentioned. To avoid zero point errors in the wavelength scale which would affect the radial velocity measurements, we have measured the position of the geocoronal Lyman α line filling-in the large aperture and, in case this line was saturated, it was measured in the small aperture taking the relative offset into account. From this test we conclude that our velocity determinations should be accurate to within ± 4 km s^{-1}, in agreement with previous studies on the IUE wavelength accuracy (see e.g. Cassatella et al. 1996).

The measured radial velocities (heliocentric) are given in Table 4 and plotted as a function of time in Fig. 5. The top panel of Fig. 5 shows the measured mean radial velocities of the SiIII] 1892.03 Å and CIII] 1908.71 Å lines. Note that the other narrow lines follow a very similar pattern. The bottom panel shows the radial velocities of the broad components of the NIV] 1486.48 Å and of the He II 1640.35 Å lines. For comparison, Fig. 5 displays also the radial velocity curve of the M star (full line) and the velocity of the center of mass of the system (dashed line) according to the orbital parameters by Kenyon et al. (1993); the vertical bars represent the times of the photometric maxima (Fernie 1985), as in Figs. 1 and 2.

We note that the radial velocity curve of the HeII broad component, unlike the other lines reported in Fig. 5, appears shifted by about + 35 km s^{-1} with respect to the velocity of the center of mass of the system. A similar shift was reported for the HeII 4686 Å line by Hutchings et al. (1975). As far as the HeII 1640 Å line is concerned, the effect appears to be due to the presence of a P Cygni profile which depresses the short wavelength wing of the emission, as shown in Fig. 6.

It clearly appears from Fig. 5 that the radial velocities of the HeII line vary in antiphase with respect to the M star companion, i.e. in phase with the hot component. Also the amplitude of the HeII radial velocity curve, of about 20 km s^{-1}, is consistent with being the forming region associated with the hot component, if the mass ratio $M_g/M_h = 4$ and the orbital parameters in Kenyon et al. (1993) are assumed (see Sect 2.).

A different behaviour is shown by the narrow emission lines, whose photometry has been discussed in Sect. 5.1. In the period 1978 - 1981, the radial velocity of the narrow lines reaches the highest values of about ± 25 km s^{-1} at spectroscopic phases 0.0 and 0.5, respectively, i.e. when the stars have the same radial velocity of the center of mass of the system.

We note in passing that the quoted results for both the broad and narrow emission lines are consistent, respectively, with the radial velocity determinations of the HeII 4686 Å and the [OIII] 4363 Å lines reported by Hutchings et al. (1975).

In the period 1989 -1995, the amplitude of the radial velocity curve for the narrow emission lines has become substantially smaller (about 15 km s^{-1}) than in 1978-1981, but the variation are still in phase with the previous. On the contrary, the radial velocity variations of the HeII line maintain the same behaviour of the previous epoch, both in terms of phase and amplitude. These observations are consistent with the substantial decrease of the mass loss rate from the hot component, as discussed in Sect. 9.

Finally, the broad component of the NIV] 1486.48 Å line is detectable only during 1978-1981. Its behaviour is similar to that of the HeII broad line, except for the larger amplitude of the radial velocity curve. In 1989-1995 the broad NIV] component was too faint to be detectable with IUE.

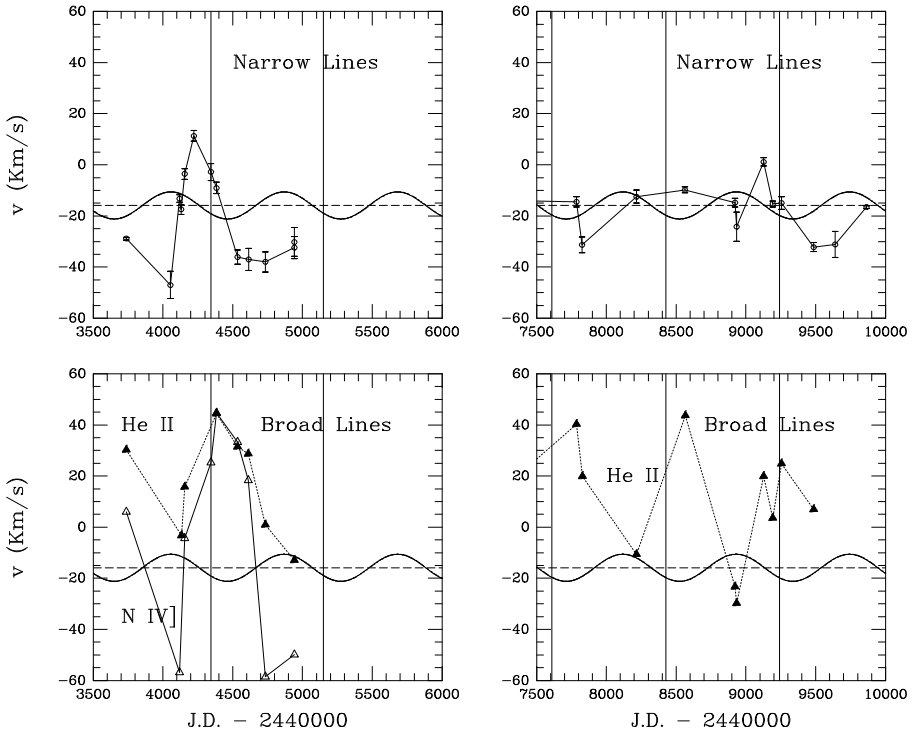

Fig. 5. Radial velocity variations of the narrow lines. Top panels: average value from the CIII] and SiIII] lines. Error bars are indicated. Bottom panels: same for the broad components of HeII 1640 Å and NIV] 1487 Å . The horizontal dashed lines represent the velocity of the center of mass. The full lines represent the radial velocity variations of the M-giant companion according to Kenyon et al. (1993).

7. The Zanstra temperature

We have estimated the temperature of the hot component of AG Peg using the Zanstra method applied to the HeII 1640 Å emission line (see Fernández-Castro et al. 1988). The assumptions implicitly made are that the emitting region is optically thick to the stellar continuum below the 228 Å ionization limit of HeII, that the HeII 1640 Å emission is optically thin, and that the hot source radiates as a black body. Under these assumptions, the Zanstra temperature T_Z can be computed from the ratio of the HeII 1640 Å line flux F(HeII) to the flux of the hot source at a suitable wavelength λ where the continuum can be measured accurately. We have selected $\lambda = 1335$ Å because it lies in a region of our spectra which is free from important emission lines and is little affected by the gas recombination continuum. In any case, the location of the continuum at 1335 Å was carefully verified in each individual spectrum to avoid systematic errors. In Table 5 we have reported for each date the *total* flux in the HeII 1640 Å line, the flux at 1335 Å (within a band 10 Å wide), the F(HeII)/F(1335) ratio and the derived Zanstra temperature.

The quoted fluxes were corrected for reddening using the extinction law by Seaton (1979) with E(B-V)=0.12. The HeII Zanstra temperature is plotted as a function of time in Fig. 7a. Filled and open dots represent measurements from low and high resolution spectra, respectively.

The results in Fig. 7a suggest that the HeII Zanstra temperature has remained nearly constant in the period 1978 - 1995, with a mean value of $86500 \pm 1300\,^{\circ}K$ (the one quoted is just the statistical error and does not include possible systematic errors due to the approximations made).

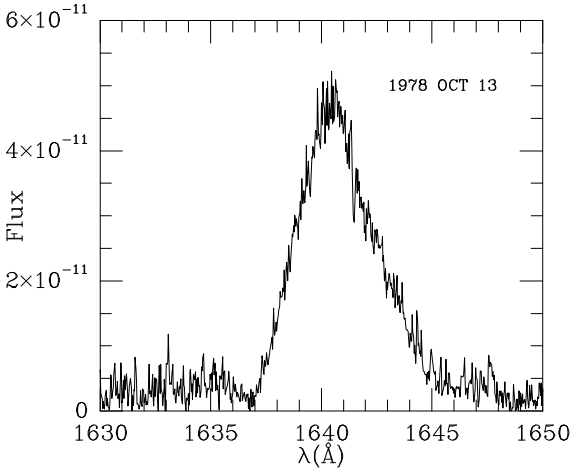

Fig. 6. Profile of an early spectrum of AG Peg showing the presence of a violet shifted P Cygni absorption.

The HeII Zanstra temperature $T_Z(HeII)$ can be considered to represent a reliable estimate of the effective temperature T_{eff} provided its value is sufficiently close to the hydrogen Zanstra temperature (Pottasch 1983). Following Fernández-Castro et al. (1988), the hydrogen Zanstra temperature $T_Z(H)$ can be estimated from the flux at, e.g., $\lambda = 2885$ Å, which is mostly contributed by the hydrogen recombination continuum, and by the flux at 1335 Å , which is mostly contributed by the hot source, here assumed to radiate as a black body. On average, the hydrogen Zanstra temperature during 1978-1995 was 75200 $\pm 10500\,^{\circ}K$, i.e. 16 % lower than the average temperature obtained through the HeII Zanstra method. The difference can be

caused by a failure in one of the assumptions made, if the hot source does not radiate as a black body and/or the nebula is not optically thick to the Hydrogen Lyman continuum (see Pottasch 1983), although also collisional contribution to the ionization balance can play a non negligible role in this case.

Since in our case the difference is within the statistical errors, $T_Z(HeII)$ can be considerd to be a fairly good approximation for T_{eff}, and we will assume this to be true in the following. The emission measure $N_e^2 V$ of the hydrogen recombination continuum, averaged over the IUE monitoring period, was $(2.6\pm0.9)\times 10^{59}$ cm^{-3}.

Two examples of how the UV reddening corrected energy distribution of AG Peg can be fitted by the sum of a hot black body and hydrogen recombination continuum are shown in Fig. 8.

Table 6. Radius, mass loss and luminosities

J.D.	$R/R_\odot$	$L/L_\odot$	F(HeII)	$\dot{M}_1$	E.W.	$\dot{M}_2$
3739	0.19	1852.8	72.80	3.72	49.13	3.98
4132	0.18	1557.9	67.10	3.43	51.16	3.63
4156	0.18	1546.5	69.10	3.47		
4385	0.17	1410.6	63.20	3.24		
4536	0.17	1320.2	59.00	3.09		
4612	0.16	1275.0	58.80	3.06	58.98	3.64
4734	0.16	1218.5	54.90	2.91	51.82	3.07
4942	0.15	1117.0	53.70	2.82	48.67	2.71
4942	0.15	1117.0	50.60	2.75		
6777	0.12	665.3	25.10	1.71	41.41	1.63
7821	0.11	584.2	14.70	1.27	33.30	1.21
7786	0.11	584.4	14.30	1.26		
8216	0.11	560.9	12.40	1.16	32.10	1.13
8565	0.11	537.9	16.20	1.31		
8921	0.10	508.8	7.80	0.89	33.81	1.10
9255	0.10	481.5	9.20	0.97	23.25	0.80
9485	0.10	448.6	9.60	0.97	27.43	0.87
9638	0.10	426.8	8.90	0.92	24.63	0.78

Note: Reddening corrected fluxes of the HeII line in Col. 4 are in units of 10^{-11} erg cm^{-2} s^{-1}.
The equivalent widths of the HeII line in Col. 6 are in Å .
The mass loss rates $\dot{M}_1$ (Col. 5) and $\dot{M}_2$ (Col. 7) refer to the optically thin and thick case, respectively, and are in units of $10^{-7}\ M_\odot$ y^{-1}.

8. Radius, luminosity and mass loss changes

Based on the previous results, we can estimate the radius of AG Peg and its variations by assuming that the reddening corrected flux at 1335 Å is due to a black body radiating at the assumed temperature of 86500 °K. The radius determinations are reported in Table 6 and shown as a function of time in Fig. 7b. From the radius and the assumed effective temperature, we have computed the bolometric luminosity L_h of the hot component $L_h = 4\pi\sigma R^2 T^4$, shown in Fig. 7c and reported in Table 6.

Kenyon et al. (1993) and Vogel and Nussbaumer (1994) have reported important changes of the luminosity and mass loss rate of the hot component during the decay phase after the 1850 outburst. Vogel and Nussbaumer (1994) have derived the mass loss rate in two ways: a) from the equivalent width, and b) from the flux of the broad component of the HeII 1640 Å line. The two determinations, although relying on opposite assumption (optically thick line in the former case and optically thin line in the latter) lead to similar values. The P Cygni profile seen in the HeII line (c.f. Fig. 6) suggests formation under optically thick conditions. However, the atomic configuration is such that, as quoted by Vogel and Nussbaumer, "the created photons are predominantly scattered and not destroyed", so that the assumptions made on the optical thickness of the line have little influence on the mass loss determination.

To derive the mass loss rate, we have adopted the same methods as Vogel and Nussbaumer (1994) and applied it to the large amount of data available. The fluxes and the equivalent widths of the HeII broad component, measured via the gaussian decomposition described in Sect. 5.2, are accurate within 15%. These measurements, together with the corresponding mass loss determinations are reported in Table 6 and plotted in Fig. 7d (dots). Our equivalent width measurements are about a factor of two smaller than those reported by Vogel and Nussbaumer (1994). We have carefully verified the continuum level around the HeII line (since its accurate location is very critical to the determination of the equivalent widths) and have also measured the equivalent widths via conventional methods in both high and low resolution spectra taken in 1978-1979, when the broad component was dominant. All these tests confirm that the equivalent widths in Table 6 are correct within the quoted errors.

9. Discussion and conclusions

We have estimated the effective temperature of the hot source in AG Peg using the Zanstra method applied to the HeII 1640 Å emission line. Kenyon et al. (1993), using the same method, derived temperatures for the hot source in the range 41700 to 95500 °K in the period 1979 to 1991. Schmutz (1996) reports 50000 °K for 1970 and 100000 °K in 1994, obtained from optical and UV data, respectively. On the contrary, Vogel and Nussbaumer (1994), did not find important variations from 1978 to 1993 and preferred to assume a constant temperature of 95000 °K. Mürset et al. (1994) reported an effective temperature of 95000 and 100000 °K in 1990 and 1993, respectively. The present study, based on many data, uniformly processed and covering a longer time span, indicates a lower temperature of 86500 °K, on average. In particular, this estimate is lower than that reported by Vogel and Nussbaumer (1994). We ascribe this difference to the systematically larger equivalent widths of the the HeII 1640 Å line reported by these authors (see Sect. 8).

The mass loss rate from the hot component was evaluated using the two methods followed by Vogel and Nussbaumer (1994) based, respectively, on the flux of the HeII line and on its equivalent width. According to the present work, the mass loss rate

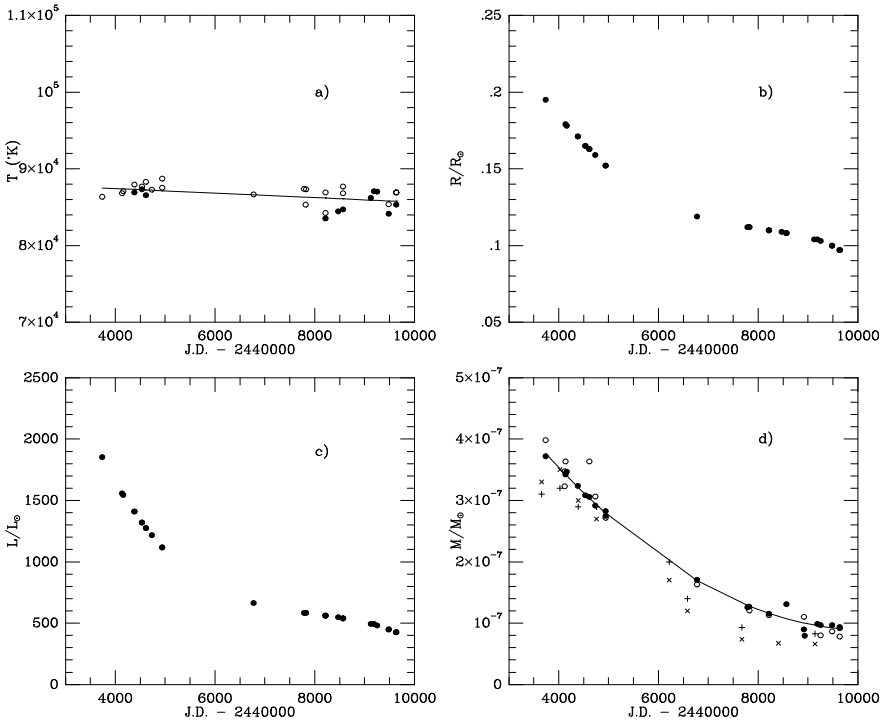

Fig. 7. Changes of the HeII Zanstra Temperature, Radius, Luminosity and Mass loss rate of AG Peg as a function of time.

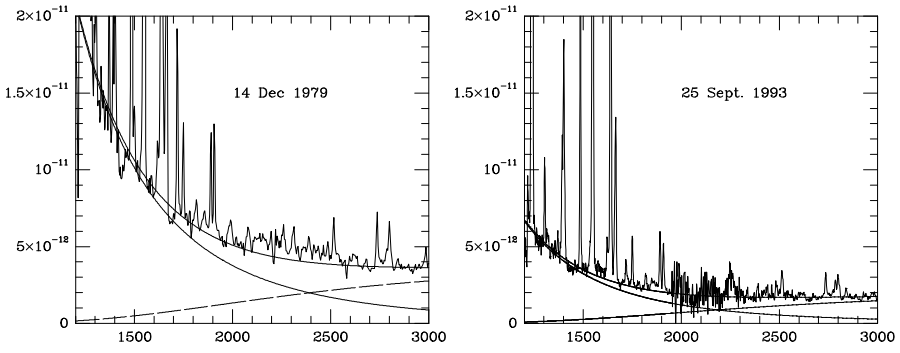

Fig. 8. The composite UV continuum of AG Peg has been represented, as shown in the figure, by the sum of a hot black body continuum with T = 86500 $^{\circ}K$(full lines) and hydrogen recombination continuum (dashed line).

has decreased from about $3.8 \times 10^{-7} M_{\odot} y^{-1}$ in August 1978 to values 4-5 times smaller in May 1995. These values are somewhat higher than the ones reported by Vogel and Nussbaumer (crosses in Fig. 7d).

As shown in Sect. 5.2, the width of the broad emission lines, and then the ejection velocity from the hot component, has remained substantially unchanged since 1978. The large decrease of the mass loss rate observed in recent years reflects then a change of the wind density, which has decreased in step with the luminosity and ionizing flux of the hot source. The observed flux decrease of the HeII and other high excitation lines is consistent with this picture.

The published profiles of the HeII 1640 Å, NV 1240 Å and CIV 1550 Å lines (Vogel and Nussbaumer 1985; Kenyon et al. 1993) suggest a common pattern for their time evolution: the broad component of the line, initially dominant, becomes fainter and fainter, until a narrow component emerges and eventually becomes the only one easily detectable. The data indicate that the broad components evolve faster the lower is their degree of ionization, as shown, e.g. by the permanence of the HeII broad component until 1995, and by the absence of it in the NIV] line at the same date (see Figs. 3a and 3b). This differential evolution explains the variety of lines profiles observed at a given time.

As described in Sect 5, the fluxes of the broad emission lines decay steadily with time in step with the UV short wavelength continuum and the luminosity of the hot source without any modulations related to the orbital motion. This fact confirms that the broad emission lines are formed in the fast wind from the hot star. In support to this view is the fact that the phase and amplitude of the radial velocity curve for the UV (this work) and optical (Hutchings et al. 1975) broad lines agree with that of the hot component.

Unlike the broad lines, the UV long wavelength continuum (dominated by hydrogen recombination continuum) and the narrow emission lines show the presence of periodic flux variations. Periodic variations are also seen in the electron density of the

narrow line region, deduced from the SiIII]/CIII] flux ratio and from the NIII] multiplet ratios (see Sect. 5.1). All these variations are in phase with the visual light curve, and can be understood in terms of reflection effects arising in the inner regions of the red giant's extended atmoshpere photoionized by the hot star (Formiggini & Leibowitz 1990). In addition, the phase-lag between the radial velocity curve of the cool star (Kenyon et al. 1993) and the light curve (Fernie 1985) suggests that the emitting region is not aligned along the axis of the system and probably asymmetric. Complex geometric situations are in fact expected in presence of colliding winds (Nussbaumer & Walder 1993; Mürset et al. 1995).

Further information on the narrow line emitting region is provided by radial velocity measurements. As shown in Sect. 6, the radial velocity curve of the narrow lines shows maxima and minima at orbital phases 0.0 and 0.5 of the M star, respectively (i.e. when the star has the velocity of the center of mass). This implies the presence of an asymmetric flow of ionized matter slowly moving out from the cool star in a direction opposite to the hot companion. Such a flow is formed by ablation of the red giant's extended atmosphere and wind by the intense ultraviolet radiation and the fast wind from the hot star. The present picture, earlier proposed by Penston and Allen (1985) on the basis of three IUE high resolution spectra obtained in 1979, is now confirmed by our analysis based on several years of monitoring.

We have found that the radial velocity curve of the narrow lines had a substantially larger amplitude in 1978 - 1981 compared to 1989 - 1995 (25 km $s^{-1}$and 15 km s^{-1}, respectively, see Fig. 5), and that the mass loss rate decreased by a factor of 4-5 from 1978 to 1995. Since the wind velocity has remained constant, its density has decreased and, after 1989, a smaller mechanical momentum was transferred to the slowly expanding envelope of the red giant. The observed smaller amplitude of the radial velocity curve for the narrow lines is then consistent with the decrease of the mass loss rate. In this model, the narrow line emitting region interests parts which, after 1989, are located deeper inside the red giant's extended atmosphere, where the density is larger. In this case, one would expect the electron density to have larger fluctuation during orbital motion in 1995 compared to 1978. Fig. 2d shows that the amplitude of the electron density variations has become larger in the last period. A the same time, also the relative amplitude of the variations in the V band, the 2885 Å band, and the narrow lines fluxes is larger in 1989-1995 (Fig. 1c,1d,2a,2b) than in the previous epoch.

Given the complex phenomenology of AG Peg and the variety of processes involved in its modeling, it would be important to continue its monitoring in the years to come, especially but not only at UV wavelengths.

Acknowledgements. We acknowledge Roberto Viotti for helpful discussions, Elio Filippetti for assisting in the preparation of the data base, and Urs Mürset for stimulating comments. This work is dedicated to the memory of Michael Penston.

References

Barylak M., 1989,ESA IUE Newsl. 33, 20

Boyarchuk A.A., 1967, Sov. Astronomy, 11, 8

Cassatella A., Fernández-Castro T., González-Riestra R., Fuensa[Blida J.J., 1992a, A&A 258, 368

Cassatella A., González-Riestra R., Imhoff C., Oliversen N., Lloyd C., 1992b, A&A 256, 309

Cassatella A., Selvelli P.L., Ponz D., Gonzalez-Riestra R., Vogel M., 1994, A&A 281,594

Cassatella A., Altamore A., Ponz J.D., Ojero, E., Talavera A., 1996, A&A Suppl., submitted

Cowley A., Stencel R., 1973, ApJ 184, 687

Fernández-Castro T., Cassatella A.,G imenez A., Viotti R., 1988, ApJ 324, 1016

Fernández-Castro T., González-Riestra R., Cassatella A., Taylor A.R., Seaquist E., 1995, ApJ 442, 366

Fernie J.D., 1985, PASP 97, 653

Formiggini L., Leibowitz E.M., 1990, 227,121

Gallagher J.S., Holm A.V.,Anderson C.M.,Webbink R.F., 1979, ApJ 229,994

González Riestra R., Cassatella A., Fernández Castro T., 1990, A&A 237, 385

Holm, A., Bohlin R.C., Cassatella A., Ponz D., Schiffer F.H., 1982, A&A 112, 341

Howarth I.D., Adams S., Snijders T., 1993, private communication

Hutchings J.B., Cowley A.P., Redman R.O., 1975, AJ 201,404

Kenyon, S.J., Milolajewska J., Mikolajewski M., Polidan, R.S., Slovak M.H., 1993, AJ 106, 1573

Munari U., 1989, A&A 208, 63

Mürset U., Nussbaumer H., Schmid H.M., Vogel M., 1991,A&A 248, 458

Mürset U., Nussbaumer H., 1994,A&A 282, 604

Mürset U., Jordan S., Walder R., 1995, A&A 297, L87

Nussbaumer H., Vogel M., 1989, A&A 213, 137

Nussbaumer H., Stencel R.E., 1987, *Exploring the Universe with the IUE Satellite*, ed. Y. Kondo, D. Reidel, p. 203

Nussbaumer H., Schmutz W., Vogel M., 1995, A&A 293, L13

Nussbaumer H., Walder R., 1993, A&A 278, 209

Penston M.V., Allen D.A., 1985, MNRAS 212, 939

Pottasch S.R., 1983, *Planetary Nebulae*, D. Reidel (Dordrecht)

Seaton M.J., 1979, MNRAS 187, 73p

Schmutz W., 1996, in *Science with the HST - II*, eds. P. Benvenuti, F.D. Macchetto, E.J. Schreier,

Viotti R., Altamore A., Baratta G.B., Cassatella A., Friedjung M., 1984, ApJ 283,226

Vogel M., Nussbaumer H., 1994, A&A 248, 145

This article was processed by the author using Springer-Verlag TEX A&A macro package version 4.